daime, a novel image analysis program for microbial ecology and biofilm research

Holger Daims,* Sebastian Lücker and Michael Wagner
Department für Mikrobielle Ökologie, Universität Wien, Althanstrasse 14, A-1090 Vienna, Austria.

Summary

Combinations of microscopy and molecular techniques to detect, identify and characterize microorganisms in environmental and medical samples are widely used in microbial ecology and biofilm research. The scope of these methods, which include fluorescence *in situ* hybridization (FISH) with rRNA-targeted probes, is extended by digital image analysis routines that extract from micrographs important quantitative data. Here we introduce *daime* (digital image analysis in microbial ecology), a new computer program integrating 2-D and 3-D image analysis and visualization functionality, which has previously not been available in a single open-source software package. For example, *daime* automatically finds 2-D and 3-D objects in images and confocal image stacks, and offers special functions for quantifying microbial populations and evaluating new FISH probes. A novel feature is the quantification of spatial localization patterns of microorganisms in complex samples like biofilms. In combination with '3D-FISH', which preserves the 3-D structure of samples, this stereological technique was applied in a proof of principle experiment on activated sludge and provided quantitative evidence that functionally linked ammonia and nitrite oxidizers cluster together in their habitat. This image analysis method complements recent molecular techniques for analysing structure–function relationships in microbial communities and will help to characterize symbiotic interactions among microorganisms.

Introduction

More than three centuries after Antonie van Leeuwenhoek manufactured the first powerful microscopes, their modern forms are still the most frequently used instruments in all fields of microbiology. In particular, microbial ecology has been boosted by novel techniques combining fluorescence microscopy with molecular methods that make it possible to detect and identify microorganisms directly in their natural habitats and to explore their physiological and genetic properties *in situ*. Prominent examples of such approaches are fluorescence *in situ* hybridization (FISH) with rRNA-targeted probes (DeLong *et al*., 1989; Amann *et al*., 1995), FISH combined with microautoradiography (Lee *et al*., 1999), immunofluorescence staining of microbial cells (Schloter *et al*., 1997), and the use of green fluorescent protein (GFP) as a reporter for monitoring gene expression and regulation (reviewed by Southward and Surette, 2002). The application range of these molecular tools was greatly extended by the integration of confocal laser scanning microscopy, which supersedes mechanical sectioning of thick specimen and opens unmatched possibilities for analysing the spatial architecture of microbial communities, for example, in biofilm (Lawrence *et al*., 1991), floc (Wagner *et al*., 1994a) and medical samples (Moter *et al*., 1998). Modern 3-D software adds capabilities for visually exploring 3-D data contained in confocal image stacks and thus greatly facilitates the understanding of complex spatial structures (Daims *et al*., 2001a; Böckelmann *et al*., 2002).

The specific, qualitative detection of uncultured microbes may be considered the basis of molecular microbial ecology, but many ecological questions can only be tackled if – in addition – the abundance, activity or distribution of these organisms is quantified. In most cases where these features are detectable by microscopy, digital image analysis can extract the quantitative data from digitized micrographs. Image analysis has been applied to quantify, for example, morphological characteristics of microbial cells (Bloem *et al*., 1995; Pernthaler *et al*., 1997; Fernandez *et al*., 2000; Liu *et al*., 2001), growth rate-related parameters (Møller *et al*., 1995), the abundance of bacterial populations as fractions of the whole microbial community (Schmid *et al*., 2000) or as absolute cell densities (Daims *et al*., 2001b; Pernthaler *et al*., 2003), the amount of fluorescence emitted by probe-labelled cells (Daims *et al*., 1999; Oerther *et al*., 2000), and biofilm structures (e.g. Kuehn *et al*., 1998; Heydorn *et al*., 2000; Xavier *et al*., 2003; Beyenal *et al*., 2004). Most of these applications were based on special macros written for existing freeware or commercial image analysis software packages, which are programmable via macro language

Received 20 April, 2005; accepted 3 June, 2005. *For correspondence. E-mail daims@microbial-ecology.net; Tel. (+43) 1 4277 54392; Fax (+43) 1 4277 54389.

interfaces. However, a stand-alone program integrating general image analysis and 3-D visualization functionality adapted to the specific needs of microbial ecology has not been available. Ideally, the use of such software would not require extensive theoretical training in image analysis or programming and would be facilitated by a graphical user interface (GUI) similar to that of well-known standard software.

Here we introduce a novel computer program for digital image analysis and visualization of microorganisms. This software, which is called '*daime*' (digital image analysis in microbial ecology), integrates image processing, image analysis and 3-D visualization features tailored to applications of FISH with rRNA-targeted probes and other fluorescence staining techniques frequently used in microbial ecology. The program works best with high-quality images acquired by a confocal laser scanning microscope (CLSM), but some functions can also be used with conventional epifluorescence, bright field or phase contrast micrographs. The whole functionality of *daime* is easily accessible from a common GUI. The goal of developing *daime* was to facilitate image analysis applications in microbial ecology by filling the gap between basic digital imaging software and larger image analysis packages designed for users willing to write their own macro programs. Here we provide an overview of the functionality of *daime* as well as more detailed descriptions of selected features for the quantification of microbial population abundance and of probe-conferred fluorescence. As technical explanations of all algorithms implemented in *daime* are beyond the scope of this report, we focus mainly on topics relevant to users of the software who lack extensive theoretical knowledge of digital image analysis.

Together with the program *daime* we present a new method for quantifying spatial localization patterns of microorganisms in complex samples and demonstrate its utility for identifying environmental biofilm microorganisms involved in mutualistic interactions. This method consists of an image analysis algorithm implemented in *daime* and a protocol to preserve the spatial structures of microbial communities during FISH with rRNA-targeted oligonucleotide probes ('3D-FISH'). In addition, the 3-D visualization capabilities of *daime* are illustrated by reconstructions of a nitrifying biofilm whose spatial structure was preserved by means of the aforementioned protocol.

Results and discussion

The diagram in Fig. 1 visualizes the tools included in the *daime* software and their interactions with each other and with the images. Differences to other software include the specific features for evaluating new FISH probes and measuring the abundance of microbial populations in environmental samples, and the capability to quantify spatial localization patterns of microorganisms. Furthermore, *daime* intensively links image analysis with 3-D visualization functionality. All image manipulation functions of the program work with temporary image copies and the user can cancel these processes before any changes made to the images are permanently stored. Once a function has altered image data, automatic notification of the other program modules ensures consistency of all image analysis and visualization operations.

Handling of image data in daime

The program *daime* reads monochrome (8 bits per pixel) and colour (RGB; 24 or 32 bits per pixel) images in the uncompressed tagged image file format (TIFF). Files in this format can be created by most imaging software,

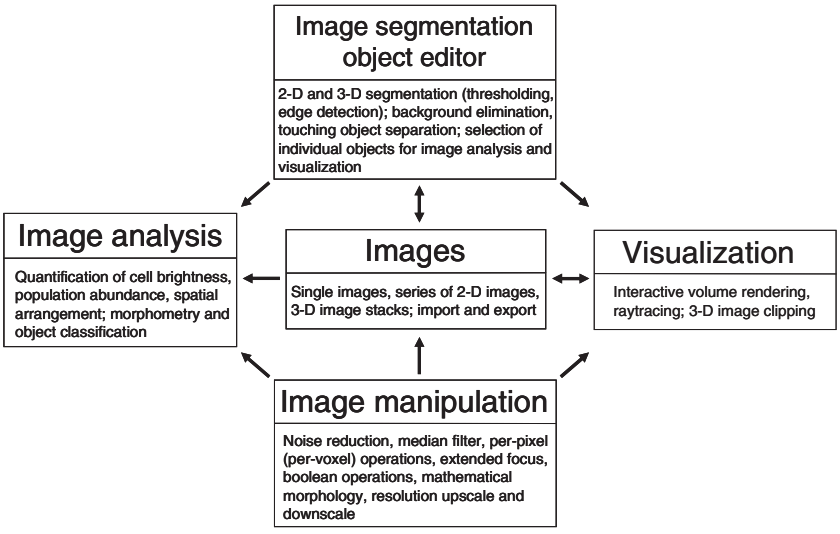

Fig. 1. The interacting modules and tools of the program *daime*.

including the programs that are delivered with the microscopes from all major manufacturers. Imported colour images are automatically prepared for separate analysis of the red, green and blue colour channels. The program imports single images as well as series of 2-D images and 3-D confocal image stacks. All functions of *daime* treat an image series or 3-D stack as a single entity, so that many images can be analysed together and with minimal need for user interaction. The number and size of imported image series and 3-D stacks are limited only by the amount of free random access memory (RAM) of the computer. The images can be exported from *daime* as TIFF files or saved to disk in a compressed file format that encodes the image data and additional information, for example, all object definitions created during image segmentation (see below). By using this feature one can store, in a single file, a complete image series together with all data needed to reproduce the results of previous image analysis or visualization sessions.

Image segmentation by daime

Analysing objects like microbial cells in images requires a pre-processing step referred to as image segmentation, which involves differentiating between objects and background and the recognition of individual objects by the computer. Image segmentation is a critical part of image analysis, as it provides the basis for all following measurements. Successful segmentation may require additional operations to enhance the quality of the image data, for example, elimination of intense background and random noise.

Due to the great diversity of analysed samples and available imaging equipment there is no gold standard approach for image segmentation of microbial cells, and different segmentation methods must usually be tested in order to obtain acceptable results with a particular image series. The program *daime* offers several options for noise reduction, background elimination and segmentation, which can easily be combined via the GUI. Well-proven methods for segmenting images of microbial cells rely on the definition of lower and upper pixel intensity thresholds, which are used to distinguish brighter objects from darker background or vice versa. However, this approach is tedious and results can be difficult to reproduce if the user must manually select the intensity thresholds. Therefore, several algorithms for automatic threshold determination have been developed (reviewed by Yang *et al*., 2001). The program *daime* automatically finds thresholds for image segmentation by using either the rapid automated threshold selection (RATS) algorithm (Kittler *et al*., 1985) or the iterative algorithm developed by Ridler and Calvard (1978). If needed, the image histogram can be used to manually refine the thresholds determined by the program. Segmentation with thresholds may fail if pronounced differences in the brightness of objects exist in the same image or if an image contains intense background. In such cases, segmentation by edge detection may perform better. This approach identifies objects by searching for discontinuities, like borders of objects, in an image. The program *daime* contains an edge detection algorithm that was derived from a method known to perform well on images of microbes (Viles and Sieracki, 1992; Ramsing *et al*., 1996). All image segmentation functions of *daime* work with single images, series of 2-D images and 3-D image stacks. According to user selection and the kind of processed image data the algorithms define either 2-D or 3-D objects. The dimensionality of the objects is automatically considered by all other image analysis tools. The user can refine the image segmentation by using an interactive object editor (Fig. 2A), which contains tools to select or reject objects for image analysis and to remove unwanted objects like autofluorescent artifacts. The object editor also has functions for entirely manual object definition and for object classification based on a few criteria (object size, brightness and shape).

Use of daime *for fluorescence intensity quantification*

The quantification of probe-conferred fluorescence after FISH with rRNA-targeted probes is one method to measure the cellular ribosome content, which may reflect the activity and growth rate of the probe target organisms (Poulsen *et al*., 1995). In cases where no direct correlation between ribosome content and physiological state can be inferred (Binder and Liu, 1998; Morgenroth *et al*., 2000), a better activity indicator may be the fluorescence intensity after FISH with probes targeting the spacer regions between the small and large subunit rRNA genes (Cangelosi and Brabant, 1997; Oerther *et al*., 2000; Schmid *et al*., 2001). Following image segmentation, the program *daime* can measure the brightness of 2-D and 3-D objects and thus offers tools useful for monitoring the *in situ* activity of microbial cells. In addition, it has special image analysis functions that help in finding the correct hybridization stringency for new rRNA-targeted probes. The optimal stringency of FISH with an rRNA-targeted oligonucleotide probe must be high enough to prevent probe hybridization to non-target organisms, but must also allow probe binding to the target organisms without significant loss of fluorescence signal. Mathematical approaches to determine these hybridization conditions (e.g. Lathe, 1985; reviewed by Stahl and Amann, 1991) provide only rough estimates, because they were developed for hybridization of nucleic acids in solution and do not take into account how rRNA secondary structures at the probe binding site and in the adjacent rRNA regions affect hybridization efficiency. Therefore, the optimal

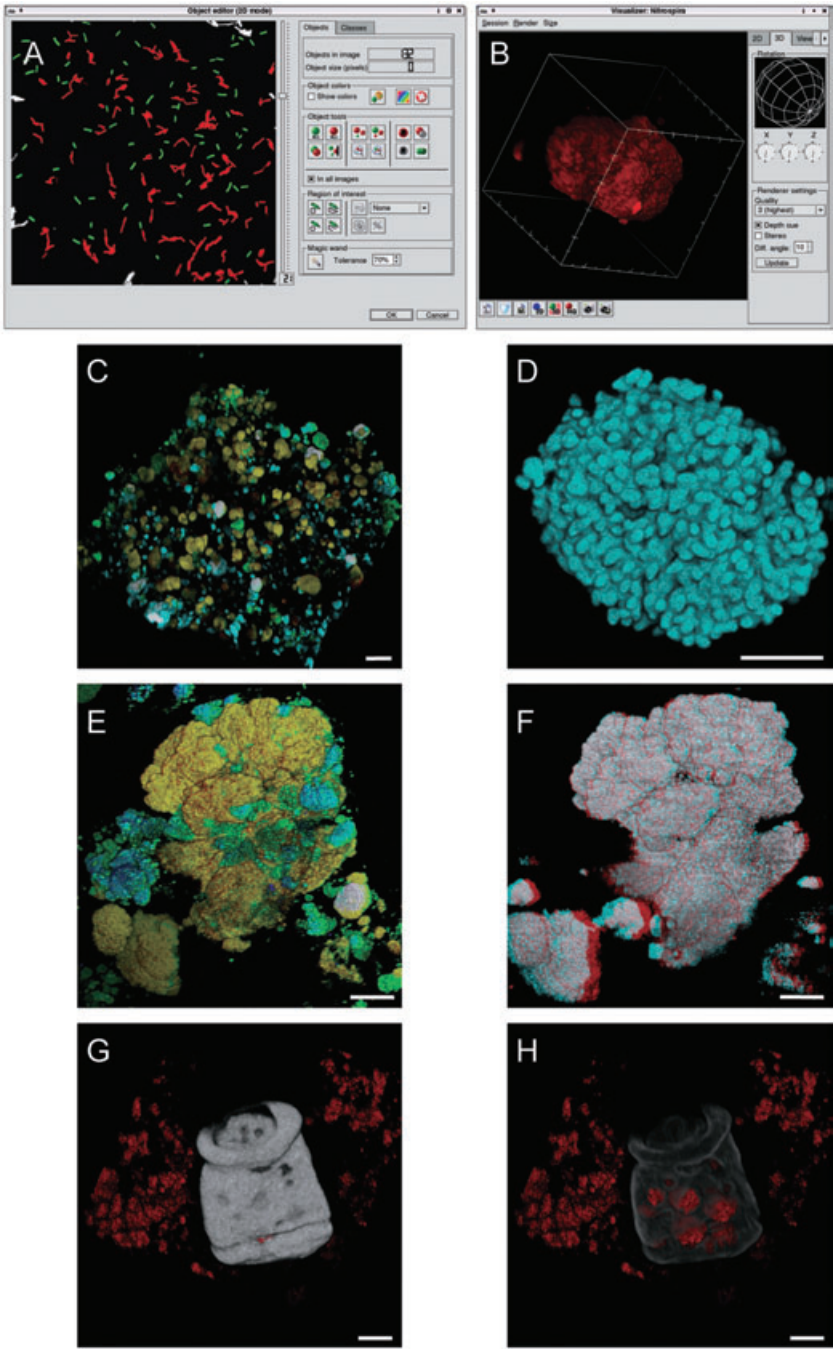

Fig. 2. Illustrations of the image segmentation and 3-D visualization features of *daime*.
A. Screenshot of the object editor. The left part of the window shows a segmented image of a bacterial pure culture. Single cells selected for image analysis are displayed green, dividing cells and cell clusters are rejected and are displayed red. White cells touch the image border and will not be analysed.
B. Screenshot of the visualization module. The central part of the window displays the 3-D reconstruction of a microcolony of *Nitrospira*-like bacteria. Also visible is the GUI for 3-D rotation and some rendering settings.
C. 3-D visualization of nitrifying biofilm hybridized to probes S-G-Ntspa-0662-a-A-18 (Cy3), S-S-Nmob-0174-a-A-18 (Cy3), S-F-bAOB-1224-a-A-20 (Cy5), S-*-Nsm-0651-a-A-18 (Cy5) and the EUB338 mix (FLUOS). Populations stained by multiple probes are *Nitrosococcus mobilis* (white), other AOB (cyan), and *Nitrospira*-like bacteria (yellow). Other *Bacteria* are displayed green. Bar = 20 μm.
D. 3-D visualization of a microcolony of AOB from the same biofilm as shown in (C) at a higher magnification. The sample was hybridized to the same probes as in (C). Bar = 5 μm.
E. 3-D visualization of the same biofilm as shown in (C) at a higher magnification. Close neighbourhood of *Nitrospira*-like bacteria and AOB is clearly visible. Bar = 10 μm.
F. Stereoscopic image of the *Nitrospira* microcolony displayed yellow in (E). Use red-green glasses for viewing (the red filter should be in front of the right eye). The image should be viewed from a distance of approximately 30 cm. Bar = 10 μm.
G. 3-D visualization of an *Epistylis* cell and surrounding bacteria in nitrifying biofilm hybridized to probes EUK516 (FLUOS; artificially coloured white) and the EUB338 mix (Cy3). The surface of the *Epistylis* cell is rendered opaque. Bar = 10 μm.
H. The same visualization as in (G), but the surface of the *Epistylis* cell is rendered semi-transparent. Bacteria inside the *Epistylis* cell are clearly visible. Bar = 10 μm.

hybridization stringency must be determined experimentally for each newly developed probe. This is accomplished by performing FISH experiments with probe target and non-target organisms and with different concentrations of formamide in the hybridization buffer and corresponding different salt concentrations in the washing buffer ('formamide concentration series', Manz *et al.*, 1992; Daims *et al.*, 2005). These experiments are evaluated either by simple microscopic observation or, much more precisely, by quantifying the brightness of the probe-labelled cells after hybridization at different stringencies. Probe dissociation profiles for target and non-target organisms are then obtained by plotting the measured fluorescence intensity against the formamide concentration. Such profiles indicate exactly how much formamide is needed to ensure specificity of the tested probe and whether an unlabelled competitor oligonucleotide is required, in addition to formamide, to prevent probe hybridization to the non-target organisms (Manz *et al.*, 1992; Wagner *et al.*, 1996).

In order to determine the optimal hybridization stringency by using *daime*, pure cultures of target and non-target organisms, or environmental samples containing such organisms, must be hybridized to the tested probe at different formamide concentrations as mentioned above. Images of at least 100 probe-labelled cells per formamide concentration are recorded by using a CLSM or an epifluorescence microscope equipped with a digital camera. When these images are imported into *daime*, the program uses the file names to automatically sort the images by formamide concentration (the file nomenclature required for this feature is described in the program documentation, which can be downloaded at http://www.microbial-ecology.net/daime). After 2-D segmentation of the images, the user can interactively select and reject cells for fluorescence intensity measurement. For example, images of a pure culture may contain not only single cells but also cell aggregates, which often appear brighter due to the higher fluorochrome density. In this case, one would prefer to measure only the single cells in order to get an unbiased probe dissociation profile. The object editor (Fig. 2A) offers several tools to select or reject objects based on their size and shape simultaneously in all images of a formamide series. Finally, *daime* measures the fluorescence intensity of each selected object, calculates the mean intensity of all objects in the images for each formamide concentration, determines the standard error of the mean and 95% confidence intervals, and displays these data together with a preview of the probe dissociation curve (Fig. 3). The results can be saved into ASCII files for use with third-party statistics and plotting software.

Application of daime *for quantification of microbial abundance*

The simplest method (at least conceptually) to measure the *in situ* abundance of bacteria is using an epifluorescence microscope for direct visual counting of cells that were specifically labelled, for example, by FISH with rRNA-targeted probes (Wagner *et al*., 1994b; Alfreider *et al*., 1996; Kämpfer *et al*., 1996; Llobet-Brossa *et al*., 1998). Direct counting works well with samples of free-living planktonic cells (e.g. in lake or marine water samples), but is extremely tedious and error-prone with large cell aggregates formed by thousands of individual cells, as typically found in biofilms or flocs. Automated counting, by image analysis, of cells in such aggregates is also difficult, because densely packed cells often touch each other and cannot easily be separated during image segmentation. This problem is partly solved in *daime* by functions to automatically split touching objects like aggregated cells. The algorithm underlying this feature is based on watershed segmentation (Serra, 1982), which is generally very efficient but also suffers from over-segmentation (unnecessary subdivision of objects).

A more generally applicable alternative to counting single cells is measuring the biovolume of a microbial population relative to the total biovolume of all microorganisms in a sample (Bouchez *et al*., 2000; Schmid *et al*., 2000; Juretschko *et al*., 2002). The biovolume fraction of any *in situ*-detectable population can be inferred from a series of 2-D images. For this purpose, a sample is simultaneously hybridized to two probes. One probe specifically targets the population to be quantified, while the second, general probe (or probe set) binds to all *Bacteria* (Daims *et al*., 1999) or to all organisms (Zheng *et al*., 1996). The second probe can be replaced by a DNA and RNA-binding dye (Schmid *et al*., 2000). The population-specific and general probes must be labelled with different fluorochromes to make their signals distinguishable. It is important to apply thick layers of sample onto the microscope slide used for FISH in order to avoid biases resulting from the accumulation of planktonic cells on the slide surface. Following FISH, at least 20 image pairs are acquired at random positions and in random focal planes so that one image

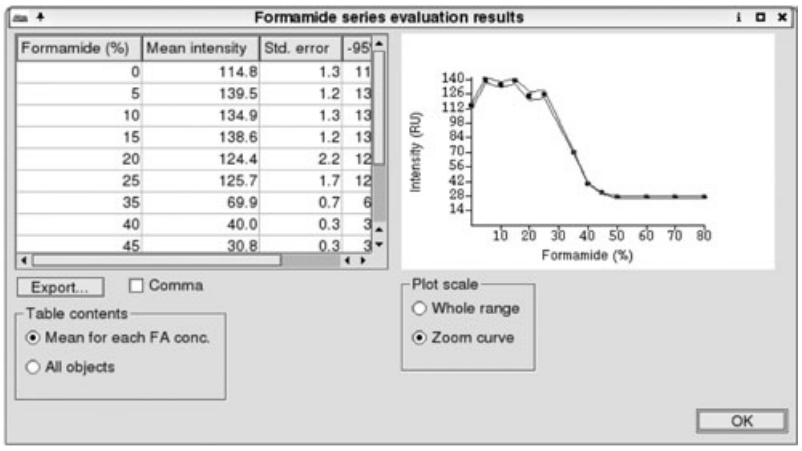

Fig. 3. Screenshot illustrating how *daime* displays the evaluation results of a formamide concentration series performed to determine the optimal hybridization conditions for a FISH probe. The table in the left part of the window contains the mean intensities of probe-conferred fluorescence measured at the different hybridization stringencies. The right part of the window shows the resulting probe dissociation profile (the markers depict the mean fluorescence intensities and the curves delimit the 95% confidence intervals).

of each pair contains only cells labelled by the population-specific probe and the other image contains cells stained by the general probe (set). The microscopic magnification should be low (e.g. 400×) to ensure that each viewing field contains sufficient biomass to achieve high quantification accuracy. The detector settings of the CLSM must be adjusted correctly to ensure that the cells of the quantified population, which should be labelled by both probes, have approximately the same size in either picture of an image pair (the images of these cells should be as congruent as possible). Following image acquisition, the areas of the cells in all images are measured by image analysis. Provided that enough image pairs are analysed, the area fraction of the cells stained by the specific probe (compared with the area of the cells labelled by the general probe) is a good estimate of the biovolume fraction of the quantified population.

The program *daime* offers an image analysis routine to quickly determine biovolume fractions. All image pairs are imported simultaneously into the program. Following 2-D segmentation of the images, the user can apply the object editor to remove autofluorescent artifacts and noise from all images. In the next step, *daime* uses the approach described above to estimate, based on all imported image pairs, the biovolume fraction V of the quantified population. The result is displayed together with some statistical parameters, which help the user to assess whether V is a good estimate of the true biovolume fraction. The program also measures the degree of congruency between the cells in the images of the specific probe signal and their counterparts in the images of the general probe signal. A low degree of congruency indicates either that the detector settings of the CLSM were incorrectly adjusted prior to image acquisition or that the image pairs still contain artifacts or noise.

The quantification approach described here has been extended to Spike-FISH, a method to determine absolute cell densities of environmental bacteria (Daims *et al.*, 2001b). Although the present version of *daime* does not directly support Spike-FISH it facilitates the use of this method, which also requires measuring biovolume fractions. The quantification of biovolume fraction could also be used, for example, to quantify bacteria stained by immunofluorescence or to determine which fraction of a population expresses a microscopically traceable reporter gene such as that coding for GFP.

Preservation and visualization of 3-D structures

The 3-D structures of environmental samples are readily distorted upon treatment according to the conventional protocol for FISH with rRNA-targeted probes (Manz *et al.*, 1992), because samples are first dried on microscope slides and subsequently dehydrated in an ethanol concentration series. As the original architecture of a sample must be preserved for visualization and quantitative analyses of 3-D spatial structures, we developed a protocol to protect sample structure during FISH by embedding the samples in polyacrylamide (PAA) gel pads. This method, referred to as '3D-FISH', was evaluated by analysing structures of activated sludge flocs and biofilms sampled from nitrifying wastewater treatment plants.

Polyacrylamide embedding had no negative consequences for FISH and did not interfere with epifluorescence and confocal laser scanning microscopy. Its autofluorescence was low and the probe-labelled cells were clearly visible in gel pads of approximately 250 μm thickness. Probe concentrations in the hybridization buffers had to be lower (1.2–2 instead of 3–5 ng μl^{-1} of each probe) and the washing step had to be longer (35 instead of 10–20 min) than in the conventional FISH protocol (Manz *et al.*, 1992) to avoid high background fluorescence due to excess probe molecules remaining in the gel pads. Despite the lower probe concentrations and the prolonged washing step, the probe target organisms were intensely labelled and clearly distinguishable from unlabelled non-target organisms and abiotic material. In an earlier study, Møller and colleagues (1998) preserved the 3-D structure of biofilms grown in flow chambers by pumping acrylamide into these chambers prior to FISH with rRNA-targeted probes. Our protocol differs in that the samples are directly applied onto silanized microscope slides. The silane covalently binds PAA (Rehman *et al.*, 1999), effectively preventing detachment of the gel pads from the slides during hybridization and washing. The embedded samples are then observed on the same slides by using an inverse CLSM equipped with a long-distance objective.

Three-dimensional visualization of nitrifying biofilms confirmed that the natural porous biofilm architecture with voids and channel-like structures between large bacterial cell aggregates was preserved during 3D-FISH, as was the integrity of the cell clusters (Fig. 2C and D). The imaging software packages delivered as bundle together with confocal microscopes often contain features to precompute and play back animated 3-D visualizations of image stacks rotated around a fixed axis of the coordinate system. In contrast, some commercial 3-D visualization programs and the 3-D visualization module of *daime* (Fig. 2B) allow free rotation around arbitrary axes and zooming of the rendered objects at interactive frame rates. The position of the virtual viewer can be freely adjusted so that one can 'walk' into a sample and look at it from arbitrary perspectives. This makes it possible to display close-ups of regions that are of particular interest, for example, where different bacterial populations occur in close neighbourhood (Fig. 2E). A special stereo rendering mode displays stereoscopic anaglyphs (Fig. 2F), which make

understanding complex 3-D structures easier. Interestingly, 3-D FISH also preserved protozoan cells of the ciliate genus *Epistylis* that we found to be major structural components of the nitrifying biofilm (Fig. 2G). In contrast, almost all *Epistylis* cells were destroyed during conventional FISH. The program *daime* can render surfaces of objects opaque or semitransparent, so that internal structures become visible. Semi-transparent visualization of *Epistylis* cells revealed bacterial cells, which could be either symbionts or prey (Fig. 2H). An obligate symbiosis between *Epistylis* and the detected bacteria is unlikely, because *Epistylis* cells without any detectable bacteria were also frequently encountered (data not shown). The dietary composition of *Epistylis* and other protozoa could be investigated in future studies by combining 3-D FISH with specific rRNA-targeted probes, 3-D visualization, and the quantitative image analysis tools of *daime*.

Spatial arrangement analysis

The use of combined molecular and optical methods, for example, FISH with rRNA-targeted probes and confocal laser scanning microscopy, has revealed a high degree of spatial organization of microbial communities. Previous studies on biofilms provided evidence that the localization of microorganisms in their habitat is determined by abiotic factors, growth requirements, and ecological interactions (reviewed by Tolker-Nielsen and Molin, 2000). For example, ammonia-oxidizing bacteria (AOB) and nitrite-oxidizing bacteria (NOB) are partners in a mutualistic symbiosis. The AOB produce nitrite, the substrate of the NOB, which in turn consume the toxic nitrite that would otherwise accumulate and inhibit the growth of AOB. Accordingly, juxtaposition of these organisms in nitrifying activated sludge and biofilm was detected by FISH (Juretschko *et al*., 1998; Okabe *et al*., 1999; Schramm *et al*., 1999). Spatial arrangement must be considered, like species composition and abundance, to be a core structural feature of microbial communities, which can directly point to yet unknown interactions between organisms in their natural habitat. To date, spatial relationships among bacteria have been analysed by qualitative microscopic observation. However, direct visual examination of selected positions in a sample is inherently biased and more subtle arrangement patterns may easily be overlooked. In order to fully exploit spatial information an objective, quantitative method to identify and compare arrangement patterns of microorganisms is required. First steps in this direction were made by Rodenacker and colleagues (2000). Nunan and colleagues (2002) used geostatistical methods to analyse spatial patterns of total bacterial density in soil, but did not extend this approach to spatial arrangement analyses of defined populations. Existing stereological approaches for quantifying microscopic architectures (e.g. Mattfeldt *et al*., 1993; Karlsson and Liljeborg, 1994) have also not been applied to analyse spatial arrangements of different microbial populations in environmental samples. Therefore, we developed a method to determine whether the spatial distribution of two microbial populations in the same confocal images is random, attractive or repulsive neighbourhood. It combines 3-D FISH with an image analysis algorithm based on a stereological approach introduced by Reed and Howard (1999) who used it to analyse animal tissues. This approach determines pair cross-correlation functions $g(r)$ of two features (for example, microbial populations) over a range of distances (r). The values of $g(r)$ indicate to what degree the analysed features are positively or negatively correlated at the different distances r: $g(r) > 1$ indicates attractive neighbourhood, $g(r) < 1$ indicates repulsive neighbourhood and $g(r) = 1$ indicates random neighbourhood of the features. One key advantage of this approach lies in its independence from the shape of the analysed features; for example, it can be applied to measure the distribution of single cells as well as that of filamentous bacteria or cell clumps. The original technique was not automated and involved manual measurement of microscopic images (Reed and Howard, 1999), but implementation of the method in software is straightforward (the algorithm is described in the *Experimental procedures*).

We applied the new method to test whether AOB and NOB in nitrifying activated sludge really cluster together as suggested by previous, qualitative observations. For this purpose, we quantified and compared the arrangement of AOB and NOB and the arrangement of AOB and green non-sulfur bacteria (GNS) in the same sludge. We chose GNS as a negative control, because to our knowledge no direct physiological link between these organisms and nitrifiers has been identified. All detectable AOB in the sludge were labelled by probe Cluster6a192, indicating that they were affiliated to the *Nitrosomonas oligotropha* lineage. All detectable NOB were labelled by probe S-G-Ntspa-0662-a-A-18 and thus were related to the genus *Nitrospira*. Members of the genus *Nitrobacter* were not detected. Probe S-*-OTU25to31-1406-a-A-18, which targets GNS, stained a morphologically diverse group of organisms containing single coccoid or rod-shaped cells and small cell clusters as well as numerous thin filaments, which penetrated the sludge flocs. The pair cross-correlation function $g(r)$ of AOB and NOB plotted against distances r between 0.6 and 150.1 μm is shown in Fig. 4F. The curve indicates attractive neighbourhood of these populations from 0.6 to 50 μm with a very high degree of clustering at short distances between 2 and 12 μm. At distances above 70 μm the values of $g(r)$ and the confidence intervals are below 1 (Fig. 4F). In a completely homogenous sample this would indicate repulsive neighbourhood of AOB and NOB as opposed to clustering at

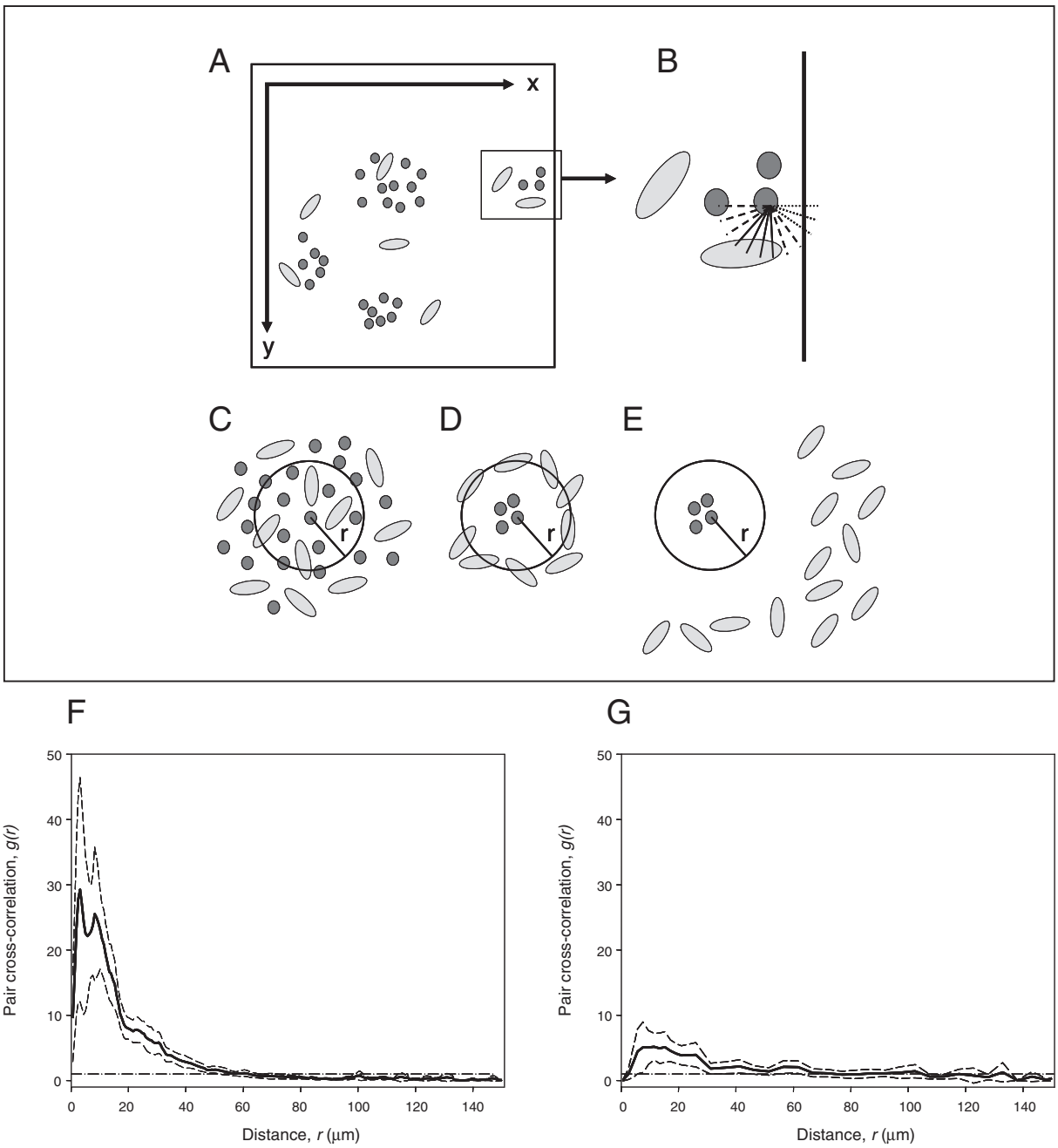

Fig. 4. A schematic diagram illustrating the operating mode of the algorithm for spatial arrangement quantification. See text for further information.
A. An image containing cells of two probe-labelled bacterial populations is scanned pixel by pixel. The arrows indicate the scanning directions along the *x* and *y* axes.
B. Magnified view of the framed area in (A) showing a semicircle of linear dipole probes extended from a pixel of the image. Dipole probes drawn as solid lines are counted as 'hits', because their ends hit both populations; dashed dipole probes are counted as 'misses', and dotted dipole probes are not counted at all because they extend the border of the image.
C. If two populations are randomly distributed, the probability that the two ends of a dipole of length *r* hit both populations is only determined by the population densities.
D. If two populations cluster together at distance *r*, the probability that the two ends of a dipole of length *r* hit both populations is greater than in (C).
E. If two populations repulse each other at distance *r*, the probability that the two ends of a dipole of length *r* hit both populations is lower than in (C).
F. Results of the spatial arrangement analysis for AOB and *Nitrospira*-like bacteria. The solid curve depicts the pair cross-correlation function for the two populations $g(r)$ averaged over all measured images. The dashed curves delimit the 95% confidence intervals of $g(r)$. The horizontal dashed-dotted line is on the level of $g(r) = 1$, which indicates random neighbourhood of the two populations at distance *r*. Values of $g(r)$ above or below this line indicate attractive or repulsive neighbourhood of the two populations respectively. $g(r)$ was estimated using Eq. (3) from estimates of covariance and population densities made using Eqs (1) and (2) respectively.
G. Results of the spatial arrangement analysis for AOB and GNS. Line styles and calculations are as described for (F).

smaller distances. However, activated sludge consists of flocs and thus is not homogenous. In the confocal cross-sections, which were used for measuring *g(r)*, the 2-D diameter of most flocs was 50–70 μm. Because AOB and NOB were found only within flocs, the observed attractive neighbourhood at distances below 50 μm was partly enforced by the floc size. Thus the apparent repulsive neighbourhood at longer distances is an artifact caused by the absence of nitrifiers outside of flocs. The curve of *g(r)* for AOB and GNS (Fig. 4G) also indicates clustering of these organisms at distances up to 50 μm. However, the peak is much lower than and not as sharp as the peak in the curve for AOB and NOB. Although we cannot completely rule out that specific biological interactions exist between AOB and GNS we propose, based on the much stronger clustering signal obtained for the symbiotic nitrifiers, that the observed clustering of AOB and GNS is a consequence of floc size rather than of a symbiotic relationship.

The results obtained for three different microbial populations demonstrate that spatial arrangement analyses can help to identify organisms involved in mutualistic (or antagonistic) interactions if proper controls are used and the physical structure of the sample is taken into account. The method described here handles two populations per single analysis, so that spatial arrangement patterns of three or more populations must be inferred by comparing the results of several pairwise analyses. In the case of nitrifiers, the physiological basis of the symbiosis is already known. If spatial arrangement analyses reveal specific localization patterns among physiologically not yet characterized organisms, molecular approaches like FISH-MAR and stable isotope probing (Lee *et al*., 1999; Radajewski *et al*., 2000; Ginige *et al*., 2004) may be used to infer the nature of the biological interactions.

Several other approaches exist for estimating pair correlation and pair cross-correlation functions from microscopic images (e.g. Philimonenko *et al*., 2000). The approach we selected as the basis of our algorithm has the advantage of being relatively tolerant to anisotropic samples with a non-random internal microstructure (Reed and Howard, 1999). Many biological samples are highly ordered and thus fall into this category. However, highly anisotropic structures like vertically stratified biofilms may require modifications of the approach described here. For example, one could restrict spatial arrangement analyses to single layers of such biofilms by recording all images at random *x* and *y* positions but in the same focal plane.

System requirements, availability and documentation

The program *daime* runs under recent distributions of the Linux operating system on common personal computer (PC) hardware. Linux installations must include the Qt® library (version 3.x, http://www.trolltech.com), the Tiff library (http://www.remotesensing.org/libtiff) and an OpenGL®-compatible graphics library like Mesa (http://www.mesa3d.org). In order to make full use of interactive 3-D visualization, the graphics hardware of the PC should be supported by the Direct Rendering Infrastructure (http://dri.freedesktop.org/wiki), which is an integral part of the XFree86 4.x windowing system (http://dri.freedesktop.org/wiki/XFree86) included in most Linux distributions. A high execution speed of *daime* requires high processor performance and sufficient memory (1 Gb RAM and 1 Gb swap space is recommended). As *daime* is a graphics-intensive application, a large display and high pixel resolution (1600×1200 or higher) are recommended.

The program *daime* is free of charge and is published under the GNU General Public License (http://www.gnu.org/copyleft/gpl.html). At the time of publication, the source code will be available on our homepage (http://www.microbial-ecology.net/daime). Documentation on how to compile the source code on a Linux system will be provided at the same site, but some familiarity with UNIX operating systems may be advantageous for a successful installation. In order to facilitate the use of *daime*, upon publication we will offer a bootable compact disk (CD) based on the Knoppix® Linux distribution (http://www.knopper.net/knoppix). This CD will contain a complete Linux system, which runs on most PCs without requiring any installation steps and without modifying installations of other operating systems on the same computer, and the *daime* executable. Special familiarity with Linux is usually not required to use such a CD. The image file of the CD can be downloaded from our homepage and must be burned onto a blank CD by using standard CD recording software. At the download site we will also provide a user manual for *daime* and information about future versions of the software, which may include new or improved functionality.

Experimental procedures

Operating systems and programming language

The *daime* software was developed using SuSE Linux versions 7.2 and 8.0 (http://www.novell.com/linux/suse). The entire source code was written in C++. The GUI is based upon the Qt® library (http://www.trolltech.com). The program uses hardware accelerated graphics to enable interactive 3-D visualization by volume rendering on standard PCs.

Sampling and fixation of activated sludge and biofilm

Activated sludge samples were taken from the nitrifying stage of a municipal wastewater treatment plant at Bruck/

Leitha, Austria. Nitrifying biofilm samples were retrieved from a pilot-scale sequencing batch biofilm reactor located at the municipal wastewater treatment plant of Ingolstadt, Germany. This reactor was described in detail by Arnold and colleagues (2000). Fresh samples were fixed in 3% (w/v) paraformaldehyde (PFA) for 3 h according to Daims and colleagues (2005) and were stored at −20°C in a 1:1 mixture of phosphate-buffered saline (PBS) and 96% (v/v) ethanol. The fixation protocol was modified for 3D-FISH (details are given below).

Fluorescence in situ *hybridization and microscopy*

Fluorescence *in situ* hybridization with rRNA-targeted oligonucleotide probes was performed according to the protocol described by Manz and colleagues (1992). The applied probes and their target organisms are listed in Table 1. The probes were 5′-labelled with the dye FLUOS [5(6)-carboxyfluorescein-N-hydroxysuccinimide ester] or with the sulfoindocyanine dyes Cy3 or Cy5. Labelled probes and unlabelled competitor oligonucleotides were obtained from Thermo Hybaid (Interactiva Division, Ulm, Germany). Images of probe-labelled cells were acquired using a CLSM (LSM 510 Meta, Zeiss, Oberkochen, Germany) equipped with two HeNe lasers (543 and 633 nm, respectively) for detection of Cy3 and Cy5 and an Ar ion laser (458, 477, 488 and 514 nm) for detection of FLUOS with excitation at 488 nm. The images were exported in the general (not manufacturer-specific) TIFF format (8 bits per pixel, monochrome, or 24 bits per pixel, RGB) by the software delivered with the microscope (Zeiss LSM 5, vs. 3.2) and were imported into *daime* for further analyses.

Embedding of environmental samples for 3D-FISH

Prior to embedding in PAA, PFA-fixed biomass was stored at −20°C in a 1:1 mixture of PBS and glycerol instead of the standard PBS: ethanol mixture, because ethanol was found to inhibit the polymerization of PAA. Ten microlitres of fixed sample and 10 μl of freshly prepared PAA stock solution [20% (w/v) PAA (37.5:1 acrylamide:methylenbisacrylamide; Bio-Rad, Munich, Germany), 0.1% (w/v) ammonium persulfate, 1% (v/v) tetramethylethylenediamine (Fluka BioChemika, Buchs, Switzerland)] were mixed carefully on the surface of a cover slip (24 × 50 mm; Marienfeld, Bad Mergentheim, Germany), which had been pretreated with Bind-Silane (Amersham Biosciences, Uppsala, Sweden). A rectangular Teflon spacer of 0.25 mm thickness was laid around the biomass on the cover slip and a microscope slide, which had been pretreated with Repel-Silane (Amersham Biosciences, Uppsala, Sweden), was put on top of the spacer in order to achieve a uniform thickness of the gel pad and to minimize exposure to oxygen during PAA polymerization. The treatment with Repel-Silane prevented adhesion of PAA to the slide surface. The PAA was allowed to polymerize for 10–15 min and the cover slip with the gel pad was carefully separated from the spacer and the microscope slide. In additional experiments, unfixed biomass was embedded in PAA as described above and subsequently immersed in 3% PFA for 1–3 h at 4°C, before two 5 min washes in PBS to remove the fixative. This treatment had no negative impact on FISH (data not shown). Dehydration of cells was achieved by immersing the cover slip with the gel pad in 50%, 80% and 96% (v/v) ethanol for 5 min each. After residual ethanol had completely evaporated, the gel pad was immediately covered with 50 μl of hybridization buffer, which was composed according to the conventional FISH protocol (Manz *et al*., 1992; Daims *et al*., 2005) and contained 60 ng of each applied Cy3- or Cy5-labelled, or 100 ng of each applied FLUOS-labelled, oligonucleotide probe. Subsequently, hybridization was carried out for 90–180 min in a humid chamber at 46°C. Following stringent washing for 35 min at 48°C, the cover slip was dipped eight times in ice-cold distilled water to remove remaining buffer salts from the gel pad. Thereupon it was immediately dried with pressurized air for 1 min, and was allowed to air-dry for an additional 10 min at room temperature. Prior to microscopy, the gel pad was covered with antifadent (Citifluor AF1, Citifluor, London, UK). The embedded sample was observed by using an inverse CLSM. In order to prevent bending of the cover slip during microscopy, the cover slip was laid upside down onto a microscope

Table 1. 16S rRNA-targeted oligonucleotide probes used in this study.

Probe	Target organisms	Reference
EUB338 probe mix	*Bacteria*	(Amann *et al*., 1990; Daims *et al*., 1999)
EUK516[a]	*Eukarya*	(Amann *et al*., 1990)
S-F-bAOB-1224-a-A-20 (Nso1225)[b]	Beta-proteobacterial AOB	(Mobarry *et al*., 1996)
S-*-Nsm-0651-a-A-18 (NEU)[b] with competitor (CTE)[c]	Most halophilic and halotolerant *Nitrosomonas* spp.	(Wagner *et al*., 1995)
Cluster6a192	*Nitrosomonas oligotropha* lineage (Cluster 6a)	(Adamczyk *et al*., 2003)
S-S-Nmob-0174-a-A-18 (NmV)[b]	*Nitrosococcus mobilis*	(Juretschko *et al*., 1998)
S-G-Ntspa-0662-a-A-18 with competitor (Comp-Ntspa-0662)[c]	Genus *Nitrospira*	(Daims *et al*., 2001a)
S-G-Nbac-1035-a-A-18 (Nit3)[b] with competitor (CNIT3)[c]	Genus *Nitrobacter*	(Wagner *et al*., 1996)
S-*-OTU25to31–1406-a-A-18	Green non-sulfur bacteria	(Juretschko *et al*., 2002)

a. Binds to 18S rRNA.
b. Well-known trivial names of some of the probes are given in brackets.
c. Labelled probes and unlabelled competitors were added in equal amounts to the hybridization buffer.
Additional information on the probes can be accessed on probeBase (Loy *et al*., 2003).

slide with a rectangular Teflon spacer of 0.25 mm thickness surrounding the gel pad.

Three-dimensional visualization

Activated sludge was embedded in PAA and hybridized to rRNA-targeted oligonucleotide probes specific for nitrifying bacteria, most known *Bacteria*, and eukaryotes (Table 1). Following FISH, 3-D confocal stacks of images containing the probe-labelled cells were recorded at selected positions. The pinhole diameters of the confocal microscope were adjusted so that each image corresponded to an optical section of 0.5–1 μm thickness. After these image stacks had been imported into *daime*, projections of the 3-D image data were calculated by the volume rendering algorithms implemented in the program. The appearance of rendered surfaces was fine-tuned by using different transfer functions for volume rendering, which are implemented in *daime*, with appropriate settings for surface opacity and shading.

Spatial arrangement analysis

The algorithm used to quantify spatial relationships between microbial populations was derived from a stereological approach introduced by Reed and Howard (1999). An image, which contains labelled cells of two different bacterial populations 1 and 2, is scanned pixel by pixel in the x and y dimensions (Fig. 4A). From every pixel a set of linear dipole probes describing a semicircle of radius r is extended (Fig. 4B). If each of the two ends (poles) of the same dipole probe touches a different population, this dipole is said to 'hit' the two populations (Fig. 4B). All other dipoles, including those that touch the same population with their two ends, are said to 'miss' the two populations (Fig. 4B). While the image is being scanned, the numbers of 'hits' and 'misses' are counted. Dipoles that extend the image borders (Fig. 4B) are ignored. The probability $P(r)$ that a dipole of length r hits the two populations is calculated from

$$P(r) = \frac{H_r}{T_r} \tag{1}$$

where H_r is the number of hits and T_r is the sum of hits and misses. If both populations are randomly distributed, $P(r)$ solely depends on the densities of the two populations in the image (Fig. 4C). The density of each population 1 and 2 is defined as

$$D_i = \frac{A_i}{A_T} \tag{2}$$

where D_i is the density of the population ($i = 1$ or $i = 2$), A_i is the cumulative area of all cells of population i in the image, and A_T is the total area of the image. For two randomly distributed populations $P(r) = 2D_1D_2$. In all other cases, $P(r)$ depends also on the type of non-random arrangement. For example, if the populations cluster together at distance r, $P(r)$ will be greater than in the case of random distribution; vice versa, $P(r)$ will be lower if the populations repulse each other at distance r (Fig. 4D and E). $P(r)$, which is an estimate of the covariance of the two populations (Reed and Howard, 1999), is already a useful statistical descriptor of spatial arrangement, although it is limited by its dependency on D_1 and D_2. Therefore, comparisons of spatial relationships between different pairs of populations based on $P(r)$ values can be difficult if the densities of these populations in the images differ. This problem is solved by normalizing $P(r)$ with D_1 and D_2:

$$g(r) \approx \frac{P(r)}{2 \cdot D_1 \cdot D_2} \tag{3}$$

where $g(r)$ is the estimated pair cross-correlation function at distance r. Accordingly, $g(r)$ is 1 if the populations are randomly distributed, greater than 1 if they cluster together at distance r, and less than 1 if they repulse each other at distance r. The algorithm determines $g(r)$ for a user-defined range of distances from r_{min} to r_{max}. The curve obtained by plotting $g(r)$ against r depicts the spatial arrangement of the two populations between r_{min} and r_{max} (Fig. 4F and G). Statistical confirmation is achieved by analysing several images, which must be acquired at random positions in the specimen. If an image series contains n images ($n > 1$), the program *daime* uses these images to calculate the mean $g(r)$ for each distance r and 95% confidence intervals using the standard deviation among the images and the Student's t-distribution for n-1 degrees of freedom. It should be noted that statistical support for $g(r)$ is weaker for larger distances r, because then more dipole probes of length r extend the image borders and are not counted. However, the use of linear dipole probes for estimating covariance and pair correlation functions has the advantage that the results are inherently corrected for edge effect bias (Reed and Howard, 1999). In its present form, the algorithm implemented in *daime* works with series of 2-D images instead of 3-D confocal image stacks. This does not compromise the results, because the applied stereological approach has been designed to use 2-D images for quantifying 3-D structures. It could be extended to work with 3-D image stacks, but then its usability on most current PCs would be fairly limited due to the large computational burden introduced by the third dimension.

In order to analyse spatial arrangements of nitrifying bacteria, activated sludge was embedded in PAA and hybridized simultaneously to probes S-G-Ntspa-0662-a-A-18 (labelled with FLUOS) and Cluster6a192 (labelled with Cy3). Preliminary experiments with probes S-F-bAOB-1224-a-A-20 and Cluster6a192 had shown that in this sludge, all AOB detected by the more general probe S-F-bAOB-1224-a-A-20 were also detectable by the more specific probe Cluster6a192 (data not shown). Following FISH, 48 confocal images containing the green (*Nitrospira*-like bacteria) and red (ammonia oxidizers) probe signals were recorded at random positions and random focal planes. The pinhole diameters of the confocal microscope were adjusted so that each image corresponded to an optical section of 1 μm thickness. After the images had been imported into *daime* the red and green colour channels were separated and the resulting two image series were 2-D segmented. The pair cross-correlation function of *Nitrospira*-like bacteria and AOB over a range of distances between 0.6 and 150.1 μm was then determined by the program. The spatial arrangement of AOB and GNS in the sludge was quantified by the same approach after FISH with probes S-*-OTU25to31-1406-a-A-18 and Cluster6a192. The results of all analyses were saved into ASCII files and the pair cross-correlation functions were plotted against the distances by using Sigmaplot vs. 8.0.

Acknowledgements

This work was partly funded by Grant LS 216 of the Wiener Wissenschafts-, Forschungs- und Technologiefonds, by Grant Schl 120/14-1 of the Deutsche Forschungsgemeinschaft, and by project A1 of Sonderforschungsbereich 411 from the Deutsche Forschungsgemeinschaft (Research Center of Fundamental Studies of Aerobic Biological Wastewater Treatment). We thank Karsten Rodenacker for fruitful discussions on the image analysis of microbes and Mike Taylor for critically reading the manuscript.

References

Adamczyk, J., Hesselsoe, M., Iversen, N., Horn, M., Lehner, A., Nielsen, P.H., *et al.* (2003) The isotope array, a new tool that employs substrate-mediated labeling of rRNA for determination of microbial community structure and function. *Appl Environ Microbiol* **69:** 6875–6887.

Alfreider, A., Pernthaler, J., Amann, R., Sattler, B., Glöckner, F.O., Wille, A., and Psenner, R. (1996) Community analysis of the bacterial assemblages in the winter cover and pelagic layers of a high mountain lake by *in situ* hybridization. *Appl Environ Microbiol* **62:** 2138–2144.

Amann, R.I., Binder, B.J., Olson, R.J., Chisholm, S.W., Devereux, R., and Stahl, D.A. (1990) Combination of 16S rRNA-targeted oligonucleotide probes with flow cytometry for analyzing mixed microbial populations. *Appl Environ Microbiol* **56:** 1919–1925.

Amann, R.I., Ludwig, W., and Schleifer, K.-H. (1995) Phylogenetic identification and *in situ* detection of individual microbial cells without cultivation. *Microbiol Rev* **59:** 143–169.

Arnold, E., Böhm, B., and Wilderer, P.A. (2000) Application of activated sludge and biofilm sequencing batch reactor technology to treat reject water from sludge dewatering systems: a comparison. *Water Sci Technol* **41:** 115–122.

Beyenal, H., Donovan, C., Lewandowski, Z., and Harkin, G. (2004) Three-dimensional biofilm structure quantification. *J Microbiol Methods* **59:** 395–413.

Binder, B.J., and Liu, Y.C. (1998) Growth rate regulation of rRNA content of a marine *Synechococcus* (cyanobacterium) strain. *Appl Environ Microbiol* **64:** 3346–3351.

Bloem, J., Veninga, M., and Shepherd, J. (1995) Fully automatic determination of soil bacterium numbers, cell volumes, and frequencies of dividing cells by confocal laser scanning microscopy and image analysis. *Appl Environ Microbiol* **61:** 926–936.

Böckelmann, U., Manz, W., Neu, T.R., and Szewzyk, U. (2002) Investigation of lotic microbial aggregates by a combined technique of fluorescent *in situ* hybridization and lectin-binding-analysis. *J Microbiol Methods* **49:** 75–87.

Bouchez, T., Patureau, D., Dabert, P., Juretschko, S., Doré, J., Delgenès, P., *et al.* (2000) Ecological study of a bioaugmentation failure. *Environ Microbiol* **2:** 179–190.

Cangelosi, G.A., and Brabant, W.H. (1997) Depletion of pre-16S rRNA in starved *Escherichia coli* cells. *J Bacteriol* **179:** 4457–4563.

Daims, H., Brühl, A., Amann, R., Schleifer, K.-H., and Wagner, M. (1999) The domain-specific probe EUB338 is insufficient for the detection of all *Bacteria*: development and evaluation of a more comprehensive probe set. *System Appl Microbiol* **22:** 434–444.

Daims, H., Nielsen, J.L., Nielsen, P.H., Schleifer, K.H., and Wagner, M. (2001a) *In situ* characterization of *Nitrospira*-like nitrite-oxidizing bacteria active in wastewater treatment plants. *Appl Environ Microbiol* **67:** 5273–5284.

Daims, H., Ramsing, N.B., Schleifer, K.-H., and Wagner, M. (2001b) Cultivation-independent, semiautomatic determination of absolute bacterial cell numbers in environmental samples by fluorescence *in situ* hybridization. *Appl Environ Microbiol* **67:** 5810–5818.

Daims, H., Stoecker, K., and Wagner, M. (2005) Fluorescence *in situ* hybridisation for the detection of prokaryotes. In *Molecular Microbial Ecology*. Osborn, A.M., and Smith, C.J. (eds). Abingdon, UK: Bios-Garland (in press).

DeLong, E.F., Wickham, G.S., and Pace, N.R. (1989) Phylogenetic stains: ribosomal RNA based probes for the identification of single cells. *Science* **243:** 1360–1363.

Fernandez, A.S., Hashsham, S.A., Dollhopf, S.L., Raskin, L., Glagoleva, O., Dazzo, F.B., *et al.* (2000) Flexible community structure correlates with stable community function in methanogenic bioreactor communities perturbed by glucose. *Appl Environ Microbiol* **66:** 4058–4067.

Ginige, M.P., Hugenholtz, P., Daims, H., Wagner, M., Keller, J., and Blackall, L.L. (2004) Use of stable-isotope probing, full-cycle rRNA analysis, and fluorescence *in situ* hybridization-microautoradiography to study a methanol-fed denitrifying microbial community. *Appl Environ Microbiol* **70:** 588–596.

Heydorn, A., Nielsen, A.T., Hentzer, M., Sternberg, C., Givskov, M., Ersboll, B.K., and Molin, S. (2000) Quantification of biofilm structures by the novel computer program COMSTAT. *Microbiology* **146:** 2395–2407.

Juretschko, S., Timmermann, G., Schmid, M., Schleifer, K.-H., Pommering-Röser, A., Koops, H.-P., and Wagner, M. (1998) Combined molecular and conventional analyses of nitrifying bacterium diversity in activated sludge: *Nitrosococcus mobilis* and *Nitrospira*-like bacteria as dominant populations. *Appl Environ Microbiol* **64:** 3042–3051.

Juretschko, S., Loy, A., Lehner, A., and Wagner, M. (2002) The microbial community composition of a nitrifying-denitrifying activated sludge from an industrial sewage treatment plant analyzed by the full-cycle rRNA approach. *System Appl Microbiol* **25:** 84–99.

Kämpfer, P., Erhart, R., Beimfohr, C., Böhringer, J., Wagner, M., and Amann, R. (1996) Characterization of bacterial communities from activated sludge: culture-dependent numerical identification versus *in situ* identification using group- and genus-specific rRNA-targeted oligonucleotide probes. *Microb Ecol* **32:** 101–121.

Karlsson, L.M., and Liljeborg, A. (1994) Second-order stereology for pores in translucent alumina studied by confocal laser scanning microscopy. *J Microsc* **175:** 186–194.

Kittler, J., Illingworth, J., and Föglein, J. (1985) Threshold selection based on a simple image statistic. *Comput Vis Graph Image Proc* **30:** 125–147.

Kuehn, M., Hausner, M., Bungartz, H.-J., Wagner, M., Wilderer, P.A., and Wuertz, S. (1998) Automated confocal laser scanning microscopy and semiautomated image pro-

cessing for analysis of biofilms. *Appl Environ Microbiol* **64:** 4115–4127.

Lathe, R. (1985) Synthetic oligonucleotide probes deduced from amino acid sequence data. Theoretical and practical considerations. *J Mol Biol* **183:** 1–12.

Lawrence, J.R., Korber, D.R., Hoyle, B.D., Costerton, J.W., and Caldwell, D.E. (1991) Optical sectioning of microbial biofilms. *J Bacteriol* **173:** 6558–6567.

Lee, N., Nielsen, P.H., Andreasen, K.H., Juretschko, S., Nielsen, J.L., Schleifer, K.-H., and Wagner, M. (1999) Combination of fluorescent *in situ* hybridization and microautoradiography – a new tool for structure–function analyses in microbial ecology. *Appl Environ Microbiol* **65:** 1289–1297.

Liu, J., Dazzo, F.B., and Glagoleva, O., Yu, B., and Jain, A.K. (2001) CMEIAS: a computer-aided system for the image analysis of bacterial morphotypes in microbial communities. *Microb Ecol* **41:** 173–194.

Llobet-Brossa, E., Rosselló-Mora, R., and Amann, R. (1998) Microbial community composition of wadden sea sediments as revealed by fluorescence *in situ* hybridization. *Appl Environ Microbiol* **64:** 2691–2696.

Loy, A., Horn, M., and Wagner, M. (2003) probeBase: an online resource for rRNA-targeted oligonucleotide probes. *Nucleic Acids Res* **31:** 514–516.

Manz, W., Amann, R., Ludwig, W., Wagner, M., and Schleifer, K.-H. (1992) Phylogenetic oligodeoxynucleotide probes for the major subclasses of proteobacteria: problems and solutions. *System Appl Microbiol* **15:** 593–600.

Mattfeldt, T., Frey, H., and Rose, C. (1993) Second-order stereology of benign and malignant alterations of the human mammary gland. *J Microsc* **171:** 143–151.

Mobarry, B.K., Wagner, M., Urbain, V., Rittmann, B.E., and Stahl, D.A. (1996) Phylogenetic probes for analyzing abundance and spatial organization of nitrifying bacteria. *Appl Environ Microbiol* **62:** 2156–2162.

Møller, S., Kristensen, C.S., Poulsen, L.K., Carstensen, J.M., and Molin, S. (1995) Bacterial growth on surfaces: automated image analysis for quantification of growth rate-related parameters. *Appl Environ Microbiol* **61:** 741–748.

Møller, S., Sternberg, C., Andersen, J.B., Christensen, B.B., Ramos, J.L., Givskov, M., and Molin, S. (1998) *In situ* gene expression in mixed-culture biofilms: evidence of metabolic interactions between community members. *Appl Environ Microbiol* **64:** 721–732.

Morgenroth, E., Obermayer, A., Arnold, E., Brühl, A., Wagner, M., and Wilderer, P.A. (2000) Effect of long-term idle periods on the performance of sequencing batch reactors. *Water Sci Technol* **41:** 105–113.

Moter, A., Leist, G., Rudolph, R., Schrank, K., Choi, B.K., Wagner, M., and Göbel, U.B. (1998) Fluorescence *in situ* hybridization shows spatial distribution of as yet uncultured treponemes in biopsies from digital dermatitis lesions. *Microbiology* **144:** 2459–2467.

Nunan, N., Wu, K., Young, I.M., Crawford, J.W., and Ritz, K. (2002) *In situ* spatial patterns of soil bacterial populations, mapped at multiple scales, in an arable soil. *Microb Ecol* **44:** 296–305.

Oerther, D.B., Pernthaler, J., Schramm, A., Amann, R., and Raskin, L. (2000) Monitoring precursor 16S rRNAs of *Acinetobacter* spp. in activated sludge wastewater treatment systems. *Appl Environ Microbiol* **66:** 2154–2165.

Okabe, S., Satoh, H., and Watanabe, Y. (1999) *In situ* analysis of nitrifying biofilms as determined by *in situ* hybridization and the use of microelectrodes. *Appl Environ Microbiol* **65:** 3182–3191.

Pernthaler, J., Alfreider, A., Posch, T., Andreatta, S., and Psenner, R. (1997) *In situ* classification and image cytometry of pelagic bacteria from a high mountain lake (Gossenköllesee, Austria). *Appl Environ Microbiol* **63:** 4778–4783.

Pernthaler, J., Pernthaler, A., and Amann, R. (2003) Automated enumeration of groups of marine picoplankton after fluorescence *in situ* hybridization. *Appl Environ Microbiol* **69:** 2631–2637.

Philimonenko, A.A., Janácek, J., and Hozák, P. (2000) Statistical evaluation of colocalization patterns in immunogold labeling experiments. *J Struct Biol* **132:** 201–210.

Poulsen, L.K., Licht, T.R., Rang, C., Krogfelt, K.A., and Molin, S. (1995) Physiological state of *Escherichia coli* BJ4 growing in the large intestines of streptomycin-treated mice. *J Bacteriol* **177:** 5840–5845.

Radajewski, S., Ineson, P., Parekh, N.R., and Murrell, J.C. (2000) Stable-isotope probing as a tool in microbial ecology. *Nature* **403:** 646–649.

Ramsing, N.B., Fossing, H., Ferdelman, T.G., Andersen, F., and Thamdrup, B. (1996) Distribution of bacterial populations in a stratified fjord (Mariager Fjord, Denmark) quantified by *in situ* hybridization and related to chemical gradients in the water column. *Appl Environ Microbiol* **62:** 1391–1404.

Reed, M.G., and Howard, C.V. (1999) Stereological estimation of covariance using linear dipole probes. *J Microsc* **195:** 96–103.

Rehman, F.N., Audeh, M., Abrams, E.S., Hammond, P.W., Kenney, M., and Boles, T.C. (1999) Immobilization of acrylamide-modified oligonucleotides by co-polymerization. *Nucleic Acids Res* **27:** 649–655.

Ridler, T., and Calvard, S. (1978) Picture thresholding using an iterative selection method. *IEEE Trans Systems Man Cybernet* **8:** 630–632.

Rodenacker, K., Brühl, A., Hausner, M., Kühn, M., Liebscher, V., Wagner, M., *et al.* (2000) Quantification of biofilms in multi-spectral digital volumes from confocal laser scanning microscopes. *Image Anal Stereol* **19:** 151–156.

Schloter, M., Wiehe, W., Assmus, B., Steindl, H., Becke, H., Hoflich, G., and Hartmann, A. (1997) Root colonization of different plants by plant-growth-promoting *Rhizobium leguminosarum* bv. *trifolii* R39 studied with monospecific polyclonal antisera. *Appl Environ Microbiol* **63:** 2038–2046.

Schmid, M., Twachtmann, U., Klein, M., Strous, M., Juretschko, S., Jetten, M., *et al.* (2000) Molecular evidence for a genus-level diversity of bacteria capable of catalyzing anaerobic ammonium oxidation. *System Appl Microbiol* **23:** 93–106.

Schmid, M., Schmitz-Esser, S., Jetten, M., and Wagner, M. (2001) 16S–23S rDNA intergenic spacer and 23S rDNA of anaerobic ammonium-oxidizing bacteria: implications for phylogeny and *in situ* detection. *Environ Microbiol* **3:** 450–459.

Schramm, A., de Beer, D., van den Heuvel, J.C., Ottengraf, S., and Amann, R. (1999) Microscale distribution of populations and activities of *Nitrosospira and Nitrospira* spp. along a macroscale gradient in a nitrifying bioreactor: quantification by *in situ* hybridization and the use of microsensors. *Appl Environ Microbiol* **65:** 3690–3696.

Serra, J. (1982) *Image Analysis and Mathematical Morphology*. New York, USA: Academic Press.

Southward, C.M., and Surette, M.G. (2002) The dynamic microbe: green fluorescent protein brings bacteria to light. *Mol Microbiol* **45:** 1191–1196.

Stahl, D.A., and Amann, R. (1991) Development and application of nucleic acid probes. In *Nucleic Acid Techniques in Bacterial Systematics*. Stackebrandt, E., and Goodfellow, M. (eds). Chichester, UK: John Wiley & Sons, pp. 205–248.

Tolker-Nielsen, T., and Molin, S. (2000) Spatial organization of microbial biofilm communities. *Microb Ecol* **40:** 75–84.

Viles, C.L., and Sieracki, M.E. (1992) Measurement of marine picoplankton cell size by using a cooled, charge-coupled device camera with image-analyzed fluorescence microscopy. *Appl Environ Microbiol* **58:** 584–592.

Wagner, M., Aβmuss, B., Hartmann, A., Hutzler, P., and Amann, R. (1994a) *In situ* analysis of microbial consortia in activated sludge using fluorescently labelled, rRNA-targeted oligonucleotide probes and confocal laser scanning microscopy. *J Microsc* **176:** 181–187.

Wagner, M., Erhart, R., Manz, W., Amann, R., Lemmer, H., Wedl, D., and Schleifer, K.-H. (1994b) Development of an rRNA-targeted oligonucleotide probe specific for the genus *Acinetobacter* and its application for *in situ* monitoring in activated sludge. *Appl Environ Microbiol* **60:** 792–800.

Wagner, M., Rath, G., Amann, R., Koops, H.-P., and Schleifer, K.-H. (1995) *In situ* identification of ammonia-oxidizing bacteria. *System Appl Microbiol* **18:** 251–264.

Wagner, M., Rath, G., Koops, H.-P., Flood, J., and Amann, R. (1996) *In situ* analysis of nitrifying bacteria in sewage treatment plants. *Water Sci Technol* **34:** 237–244.

Xavier, J.B., White, D.C., and Almeida, J.S. (2003) Automated biofilm morphology quantification from confocal laser scanning microscopy imaging. *Water Sci Technol* **47:** 31–37.

Yang, X., Beyenal, H., Harkin, G., and Lewandowski, Z. (2001) Evaluation of biofilm image thresholding methods. *Water Res* **35:** 1149–1158.

Zheng, D., Alm, E.W., Stahl, D.A., and Raskin, L. (1996) Characterization of universal small-subunit rRNA hybridization probes for quantitative molecular microbial ecology studies. *Appl Environ Microbiol* **62:** 4504–4513.